THE ASTROPHYSICAL JOURNAL, 419:725–732, 1993 December 20

THE 150 AU STRUCTURE OF THE RADIO CONTINUUM AND THE AMMONIA BIPOLAR OUTFLOW IN CRL 618

JESÚS MARTÍN-PINTADO,[1] RALPH GAUME,[2] RAFAEL BACHILLER,[1] AND KEN JOHNSTON[2]
Received 1993 March 12; accepted 1993 June 28

ABSTRACT

We present high angular resolution (0.″096 × 0.″066) observations of the radio continuum emission at 23 GHz and of the (2, 2) line of NH_3 toward the protoplanetary nebula CRL 618. The integrated flux density in the continuum indicates that the source has not experienced any systematic increase since 1980. The continuum emission is elongated in the east–west direction and shows an elliptical shell structure, reminiscent of an extremely young planetary nebula. While the southern part of the elliptical shell is rather uniform, the northern portion shows clumpy structure. The walls of the shell are unresolved by our 0.″066 beam. The continuum structure indicates that the H II region is not isothermal, but the electron temperature increases toward the edges.

Ammonia is detected only in absorption toward the continuum source. The deepest absorption occurs at -50 km s^{-1}, blueshifted with respect to the radial velocity of the approaching part of the expanding envelope (about -40 km s^{-1}). The ammonia lines show a bipolar distribution with the blueshifted (radial velocities $\lesssim -45$ km s^{-1}) and redshifted (radial velocities $\gtrsim -45$ km s^{-1}) absorptions found toward the eastern and western parts of the H II region, respectively. The most blueshifted gas is found at the eastern edge of the continuum source, possibly indicating that acceleration of the high-velocity gas is taking place at scales of a few 100 AU. The optical depth of the absorption lines is not uniform, but increases from the center to the western and eastern edges of the H II region. The data indicate that the ammonia absorption does not arise in the slow expanding asymptotic giant branch (AGB) envelope, but from the high-velocity molecular outflow. The NH_3 fractional abundance increases by more than three orders of magnitude from $\lesssim 8 \times 10^{-9}$ in the AGB envelope to at least 2×10^{-5} in the molecular outflow. The chemistry of NH_3 in protoplanetary nebulae is briefly discussed.

Subject headings: H II regions — ISM: individual (CRL 618) — ISM: jets and outflows — ISM: kinematics and dynamics — planetary nebulae: general — radio continuum: interstellar

1. INTRODUCTION

It is well established that planetary nebulae are formed from red giants once the central star becomes hot enough to ionize the circumstellar envelope. However, the physical processes involved in the formation, shaping, and evolution of planetary nebulae are poorly known (see, e.g., Pottasch 1984). In order to ascertain the predominant mechanism (ionization after the superwind phase, sudden ejecta, and interacting winds), one must make more detailed studies of objects in the protoplanetary stage. The major problem related to this kind of study is the lack of known objects in this elusive phase of stellar evolution. At a distance of 1.7 kpc, the protoplanetary nebula (PPN) CRL 618 is one of the best candidates to study the formation of planetary nebulae. It shows the characteristics of an evolved star in the red giant stage, namely strong emission in a large variety of molecules arising from a slow, 20 km s^{-1}, expanding envelope remnant of the asymptotic giant branch phase—hereafter AGB envelope—(Zuckermann et al. 1977; Bachiller et al. 1988; Bujarrabal et al. 1988), and has the properties of a nascent planetary nebula: a time-variable ultracompact H II region (Westbrook et al. 1975; Kwok and Feldman 1981; Spergel, Giuliani, & Knapp 1983; Martín-Pintado et al. 1988; Walmsley et al. 1991). In addition to these characteristics, CRL 618 also shows a bipolar outflow of diffuse ionized gas from the central star to the optical lobes (Calvet & Cohen 1978; Carsenty & Solf 1982) and the presence of H_2 vibrationally excited emission (Beckwith, Beck, & Gatley 1984; Burton & Geballe 1986). Furthermore, molecular observations have revealed the presence of very energetic molecular outflows with terminal velocities of up to 200 km s^{-1} (Cernicharo et al. 1989; Gamie et al. 1989). Mapping of the high-velocity molecular outflow with an angular resolution of 2″ barely resolves the redshifted and blueshifted emissions, indicating the outflow to be bipolar in the east–west direction (Neri et al. 1992). They conclude that the high-velocity molecular gas is produced by the impact of a primary wind from the central star on a few well-localized dense clumps in the inner envelope.

Recently, Martín-Pintado & Bachiller (1992, hereafter MB) have detected ammonia absorption and emission toward the continuum source in CRL 618. The absorption is observed in all metastable lines from the (1, 1) to the (7, 7). Two velocity components are clearly distinguished: the broad absorption (line width of ~ 25 km s^{-1}) at a radial velocity of -56 km s^{-1} and the hot core (line width of 3 km s^{-1}) at a radial velocity of -28 km s^{-1}. Both components arise from hot gas with kinetic temperatures of, at least, 150 and 270 K, respectively. Based on kinematical arguments, MB have proposed that both com-

[1] Centro Astronómico de Yebes (IGN), Apartado 148, 19080-Guadalajara, Spain.
[2] Remote Sensing Division, Naval Research Laboratory, Washington, DC 20375-5351.

ponents correspond to the high-velocity gas of the molecular outflow in front of the H II region. In particular, the hot core and its unusual radial velocity have been interpreted as a clump which has been torn off from the inner circumstellar envelope by the stellar wind and now participates in the high-velocity molecular outflow.

The VLA is the only instrument which provides the angular resolution (well below 1″) and the sensitivity required to study in detail the characteristics (bipolarity, clumping, acceleration, kinetic temperature, molecule formation in the postshocked clumps, etc.) of the molecular outflow in CRL 618. In this paper we present the first maps of the high-velocity outflow in the (2, 2) line of NH_3 toward CRL 618 at an angular resolution of 0.″096 × 0.″066 (0.″066 = 130 AU at a distance of 1.7 kpc).

2. OBSERVATIONS

The observations occurred 1990 March 29 in the spectral line mode of the VLA.[3] All available antennas were used in the A-array which provides baseline lengths from 0.7 to 36 km. The observations of CRL 618 were centered at $\alpha(1950) = 4^h39^m34^s.03$, $\delta(1950) = 36°01'15''.9$. The source 3C 84 was used as a flux density, phase, and bandpass calibrator. The observing sequence consisted of a 15 minute scan of CRL 618 followed by a 4 minute scan of 3C 84 repeated throughout the 3 hr duration of the run. The VLA spectral line system was used in a single IF mode. The total bandwidth of the IF was 12.5 MHz. The IF was separated into 32 channels. The first channel was a wide-band channel with a width of 9.4 MHz. The remaining 31 Hanning smoothed narrow channels were each 391 kHz wide (4.9 km s^{-1}). On-line autocorrelation normalization was used to improve the amplitude portion of the bandpass. Channel 16 of the 31 narrow channels was tuned to the frequency of the $(J, K) = (2, 2)$ inversion transition of the NH_3 molecule (23.722631 GHz) at an LSR velocity, V_{LSR}, of -30 km s^{-1}.

[3] The VLA is a telescope of the National Radio Astronomy Observatory (NRAO) which is operated by Associated Universities, Inc., under cooperative agreement with the National Science Foundation.

The AIPS software package of the NRAO, as implemented on NRL computer systems, was used to calibrate, reduce, and analyze the data. The flux density scale was set by assuming a flux density of 28 Jy for the calibrator 3C 84. Antenna gain solutions were improved through the application of a self-calibration algorithm operating on the wide-band channel. The improved antenna gains were applied to the entire spectral line data set. The data for all channels were edited and transformed into 256 by 256 pixel images (pixel size 0.″02). Two sets of channel images were made. One with natural weighting of the data in the *u-v* plane, and the other with uniform weighting. Natural weighting of the data typically results in greater sensitivity, at the cost of degraded resolution. A mean continuum image was constructed from a total of four narrow-line channels. Two channels at the redshifted end of the bandpass (center velocity of 44.1 and 39.1 km s^{-1}) and two channels at the blueshifted end of the bandpass (center velocity of -89.2 and -94.2 km s^{-1}) were averaged. The mean continuum image was subtracted in the image plane from all line channels to produce a "line only" data cube. The effect of beam sidelobes was removed from the line-only data with a beam deconvolution algorithm. The FWHM beam size of the resulting images was 0.″096 × 0.″066, P.A. = $-85°$ (uniform weighting) and 0.″157 × 0.″103, P.A. = $-71°$ (natural weighting).

3. RESULTS

3.1. *Radio Continuum Emission at* 23 GHz

Figure 1 shows the radio continuum emission obtained from the uniform weighted data. The overall distribution is similar to that obtained by Kwok & Bignell (1984). The integrated flux density in the map, 189 ± 20 mJy, is also in good agreement with previous measurements (Kwok & Feldman 1981; Spergel et al. 1983; Martín-Pintado et al. 1988) and indicates that the source has not experienced any systematic increase since 1980. This is in contrast with the 1.3 mm emission which seems to show important changes from 1987 to 1990 (Walmsley et al. 1991). The better sensitivity of our map and the favorable beam shape (0.″096 × 0.″066, P.A. = $-85°$) reveals for the first time the inner structure of the nascent planetary nebula. The contin-

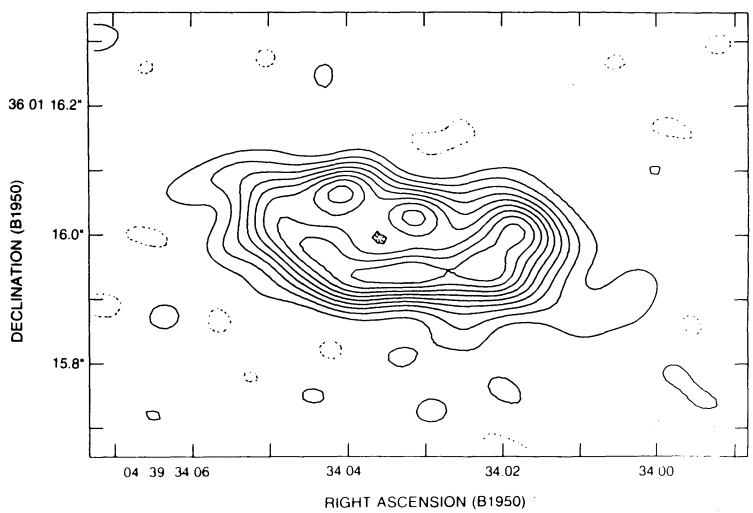

FIG. 1.—Map of the radio continuum emission of CRL 618 at 23 GHz. The contour intervals are -10, 10, 20, ..., 90% of the peak flux density of 16.7 mJy beam^{-1}. This image was obtained with uniform weighting of the *u-v* data and has a FWHM restoring beam of 0.″096 × 0.″066, P.A. = $-85°$.

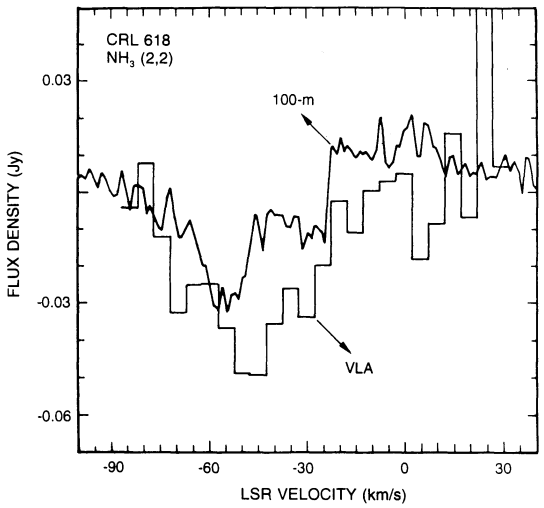

FIG. 2.—Profiles of the (2, 2) line of NH_3 as measured with single-dish telescope and the VLA (*histogram*). The VLA profile has been obtained by averaging the line emission over the radio continuum emission, and the single-dish data have been taken from MB.

uum map shows an elliptical shell with a size of 0.″40 × 0.″12. While the southern part of the shell is rather uniform, the northern portion shows clumpy structure. The flux density ratios between the edges and the center are 1.2–1.6. The shell walls seem to be unresolved in declination by our 0.″066 beam. Since the radio continuum is known to be optically thick up to 100 GHz (Martín-Pintado et al. 1988), the brightness temperature must be close to the electron temperature in the H II region. The peak main beam brightness temperature in the shell is ~7000 K; a factor of 1.7 smaller than the LTE electron temperatures derived from recombination lines at millimeter wavelengths (Martín-Pintado et al. 1988). The errors in the determination of the LTE electron temperatures derived from recombination lines at mm wavelengths are basically dominated by the uncertainties in the side band rejection. Assuming typical values and uncertainties in the image rejection (8 ± 2 dB) would account for an error in the LTE electron temperatures of ~30%. One possible explanation for the low electron temperatures derived from the radio continuum map at 23 GHz might be the small thickness of the shell, which is unresolved by our beam. Assuming that both the electron temperature derived from the mm wavelength observations and

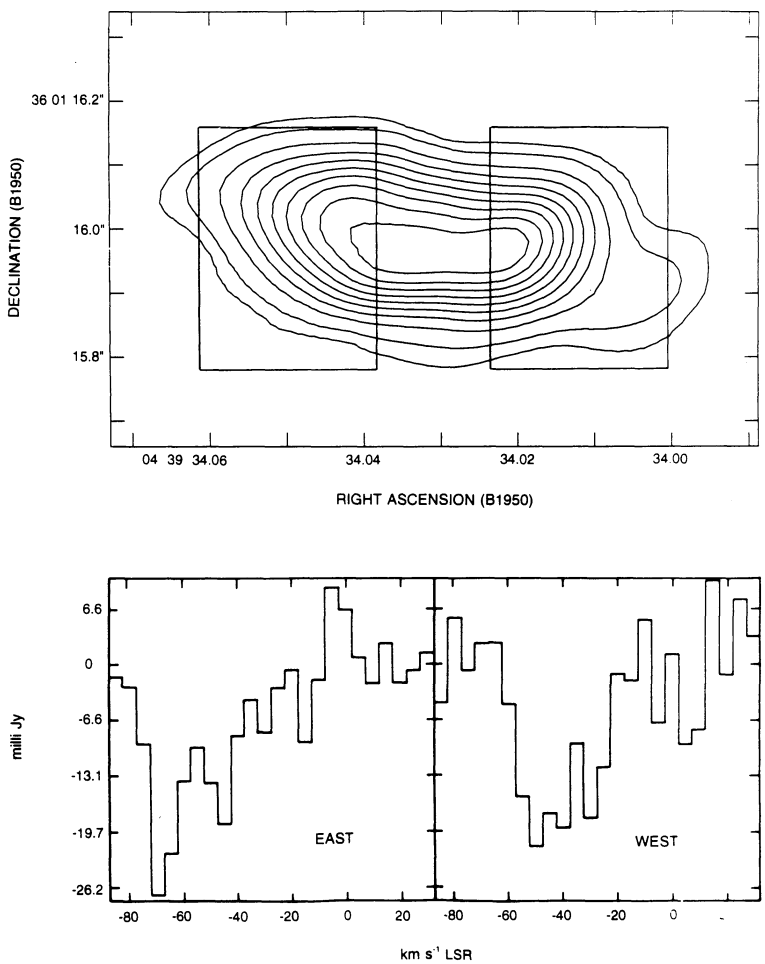

FIG. 3.—The radio continuum map of CRL 618 obtained by natural weighting the *u-v* data is shown in the upper panel. The contours are −5, 5, 10, 20, ..., 90% of the peak flux density of 35.1 mJy beam^{-1}. The rectangular areas represent the regions where the line data have been averaged to obtain the profiles of the (2, 2) line of NH_3 shown in the lower panel. The FWHM of the restoring beam is 0.″157 × 0.″103, P.A. = −71°.

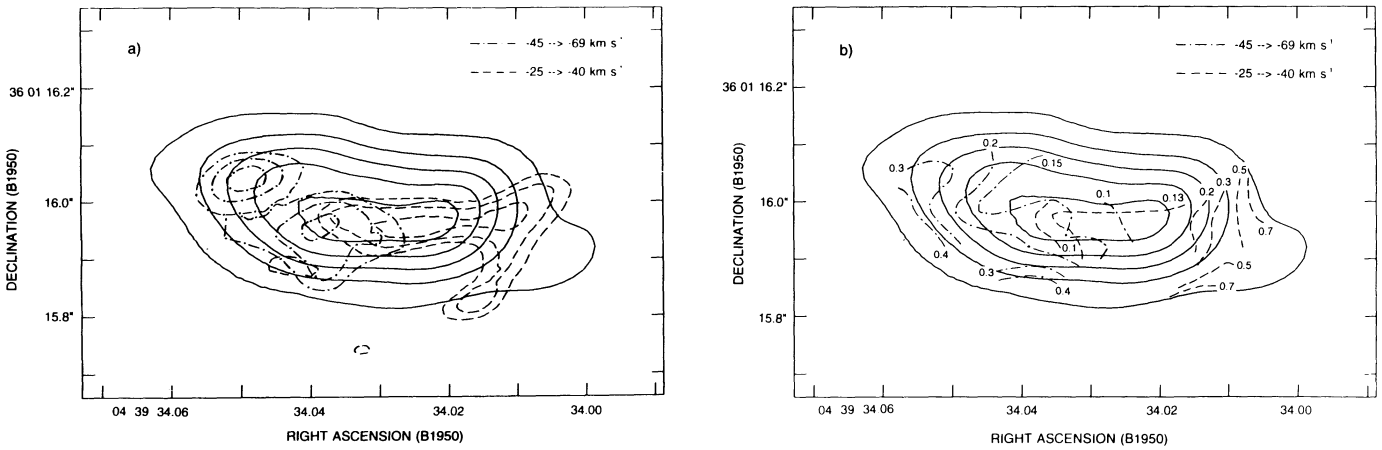

FIG. 4.—(*a*) Spatial distribution of the blueshifted (*dot-dashed*) and redshifted (*dashed*) NH_3 (2, 2) absorption line toward CRL 618 superposed on the radio continuum emission (*solid contours*). The blueshifted and redshifted absorptions have been obtained by integrating from -69 to -45 km s^{-1} and from -40 to -25 km s^{-1}, respectively. The contour levels for the continuum are 10, 30, 50, 70, 90% of the peak flux density of 35.1 mJy beam^{-1}. The contour levels for the redshifted and blueshifted absorption are 60, 70, 90% of -89.8 mJy beam^{-1} km s^{-1} and -172.8 mJy beam^{-1} km s^{-1}, respectively. The uncertainty in the line-to-continuum ratio at the edges is ≈ 0.1. (*b*) Contour lines of the velocity averaged line to continuum ratios for the redshifted and blueshifted NH_3 superposed on the radio continuum emission (see Fig. 4*a*). Each contour line is labeled with the appropriate line-to-continuum ratio.

the 1.3 cm flux density are correct, the thickness of the shell should be $\sim 0''.035$.

3.2. *The* (2, 2) *Line of* NH_3

In Figure 2 we show the line profile of the (2, 2) line of NH_3 integrated over the continuum emission as observed by the VLA superposed on the single-dish spectrum. The single-dish NH_3 data show a very complex profile with a mixture of absorption and emission features (see MB). We have clearly detected the broad absorption (BA in the MB terminology) at about -50 km s^{-1}. However, the limited velocity coverage and the sensitivity of our observations did not allow the detection of the weaker and broader emission line seen in the single-dish observations. The VLA profile seems to be deeper than the single-dish profile for radial velocities between -30 and -60 km s^{-1}. Such differences are expected if the emission arises in a more extended region than the absorption, and therefore is resolved out by the VLA. However, better sensitivity VLA data would be required to conclude if the differences between the single-dish and the VLA profiles are significant. In any case, the VLA line data seem to contain all the flux density for the BA component.

Single-channel maps show the spatial distribution of the NH_3 absorption changing with radial velocity. There is a systematic trend for the absorption to be located toward the western part of the H II region for $V_{LSR} \gtrsim -45$ km s^{-1} and to the eastern part for $V_{LSR} \lesssim -45$ km s^{-1}. Figures 3 and 4 clearly illustrate the bipolar structure of the ammonia absorption. In the lower panel of Figure 3 we show the line profiles toward the eastern and western edges of the H II region. To improve the signal-to-noise ratio, the profiles in this figure were produced by integrating the line absorption over the rectangular areas shown in the top panel of Figure 3. These lines show that absorption with $-69 \lesssim V_{LSR} \lesssim -45$ km s^{-1} and with $-40 \lesssim V_{LSR} \lesssim -25$ occurs only in the eastern and western parts of the radio continuum emission respectively. Figure 4*a* shows the spatial distribution of the blueshifted and redshifted material in front of the H II region. It is remarkable that the bipolarity is not found with respect to the systemic velocity of the central star, -20 km s^{-1}, but with respect to the terminal velocity of the expanding asymptotic giant branch (AGB) envelope in front of the H II region. The data also show hints of larger radial velocities as one moves away from the center of the H II region. Figure 4*b* shows the spatial distribution of the line-to-continuum ratio. The line-to-continuum ratio of the blue and redshifted NH_3 is far from uniform. It increases from 0.1 at the center to 0.4–0.7 at the east and western edges and also shows the presence of small-scale structure (clumps) especially in the blueshifted lobe. Since the lines are optically thin, the effects of the hyperfine components (only 5% of the main line) on the shape of the profile are negligible. Then, the shape of the line profiles must be dominated by the kinematics in CRL 618.

4. THE NASCENT PLANETARY NEBULAE SHELL

CRL 618 provides a unique opportunity to study the physical processes taking place at the birth and the first evolutionary stages of planetary nebulae. Therefore the understanding of the structure, the physical conditions, and the kinematics of this compact planetary nebula is very important for the comprehension of this elusive phase of the stellar evolution. The bipolar morphology of the H II region suggests that the ionized material is ionization bounded in declination as a result of an anisotropic density distribution in the circumstellar envelope (Kwok & Bignell 1984). Two models have been proposed to explain the characteristics of the radio continuum emission of CRL 618: a core-halo structure (Kwok & Bignell 1984), and an isothermal ionized stellar wind with an empty cavity around the star (Martín-Pintado et al. 1988). While the core-halo model explained the different sizes of the H II region in R.A. measured at different centimeter wavelengths with the VLA (Kwok & Bignell 1984), the ionized wind with a cavity was invoked to explain both the size-frequency dependence and the entire radio continuum spectrum from 1.4 to 230 GHz. The map in Figure 1 is inconsistent with the core-halo model, which predicts that most of the flux density at 23 GHz should arise from the core, and supports the ionized stellar wind model. In fact, the predicted size for the empty cavity and the thickness of the shell, $0''.082$ and $0''.028$, respectively (Martín-Pintado et al. 1988), are consistent with the values derived from

the continuum map. However, this model fails to explain the observed inner structure. In the isothermal stellar wind model the continuum emission arises in a cylinder of ionized gas with an empty cavity around the star, constant electron temperature, and a electron density law which varies like r^{-2}. At 23 GHz, the continuum emission is optically thick in declination, and any small-scale structure changes in the H II region are not related to density variations, but to electron temperature differences. This would indicate that the stellar ionized wind is not isothermal, requiring the electron temperature to increase toward the outer parts.

Model calculations of the ionization and the thermal equilibrium in a idealized spherical H II region with constant electron density (see Rubin 1968) show that, as one moves away from the star, the electron temperature first decreases smoothly and then increases toward the edges of the H II region reaching values even larger than near the star. The ratios of the electron temperatures at the center and at the edges are similar to those observed in CRL 618. The electron temperature increase which occurs sharply and is restricted to a thin outer shell (its thickness is only 20% of the Strömgren radius), is related to the UV radiation hardening produced by the frequency dependence of the photoionization absorption cross section of hydrogen. The radiation with frequencies near to the series limit is strongly attenuated close to the star and the higher energy UV photons penetrate further into the gas (see, e.g., Osterbrook 1989). This produces an increase of the mean energy of the photoelectrons with radius, resulting in an increase in the electron temperature with radius. Electron density variations (i.e., different cooling functions) within the H II region might affect the profile of the electron temperature (Rubin 1968). However, the critical densities of collisional de-excitation for most of the main coolant lines in H II regions are, $\lesssim \times 10^6$ cm^{-3}, smaller than typical electron densities in CRL 618, $\sim 7 \times 10^6$ cm^{-3} (Martín-Pintado et al. 1988) and the expected density variation between the inner radius of the H II region and the outer one are within a factor of 2.7. Under these conditions one can approach the cooling function within CRL 618 to that of the constant density case.

To check if a simple model can reproduce the observed structure, we have considered a modified version of the model of Martín-Pintado et al. (1988) which also incorporates electron temperature variations. For simplicity, we consider that the electron temperature jumps at a given radius. Using cylindrical geometry, a density law $n \propto r^{-2}$, a mass-loss rate of $2.7 \times 10^{-5}\ M_\odot$ yr^{-1} and sizes as in Martín-Pintado et al. (1988), we are able to obtain similar brightness temperature variations to those observed if the electron temperature changes from 8000 at the center to 12,000 K at a thin outer shell of thickness 6×10^{14} cm (0".020). (The electron temperatures are larger than those inferred from the continuum map, but they fit the intensity of the H35α line; Martín-Pintado et al. 1988.) Hence, the shell-like structure observed in the radio continuum emission of CRL 618 seems to be consistent with temperature gradients within the H II region which qualitatively are expected from simple theoretical models of H II regions.

5. NH_3 IN THE AGB CIRCUMSTELLAR ENVELOPE

The data presented in this paper indicate that the NH_3 abundance in the AGB envelope is low. If NH_3 were abundant in the AGB envelope, one should not observe similar line profiles with the VLA and single dish because each instrument samples quite different spatial scales of the envelope. While the single-dish profile should be dominated by the emission of the extended ($\sim 10''$) AGB circumstellar envelope, the VLA data should sample only the material located in front of the H II region. Furthermore, the line profiles and the spatial distribution of the absorption lines observed with the VLA are also inconsistent with the NH_3 absorption arising only from the AGB envelope. The precise line shape of the lines arising from the AGB envelope will depend on the orientation of the elongated H II region, the inner radius, the internal motions, and the density and kinetic temperature distributions within the AGB envelope (see, e.g., Young et al. 1992). In the following discussion we will assume that the elongated H II is tilted 45° with respect to the line of sight (Carsenty & Solf 1982) as sketched in Figure 5. If the AGB envelope is expanding from the center of the H II region, only redshifted gas with respect to the terminal velocity, -40 km s^{-1} should be observed in absorption at both sides of the H II region. These expectations are inconsistent with the observed velocity gradients and the NH_3 profiles. The deepest NH_3 absorption is not found as expected at roughly -40 km s^{-1}, but at -50 km s^{-1}, the absorption lines are broad and extend up to radial velocities of -80 km s^{-1} which are forbidden for material in the AGB envelope, and the spatial distribution of NH_3 is bipolar. Though some of the redshifted absorption to the west might come from the AGB envelope, the data do not show its counterpart to the east. These facts imply that ammonia cannot be very abundant in the AGB envelope.

Assuming that the ammonia absorption from the AGB envelope has similar line width and radial velocity to that of HCO^+, we can set an upper limit from our data to the optical depth of the (2, 2) line in the AGB envelope of $\sim 7 \times 10^{-2}$. The intensity of the $J = 1 \rightarrow 0$ HCO^+ absorption line is similar to that of the radio continuum indicating this line to be optically thick. In the following estimates we will consider a lower limit of 1 to the optical depth for this line. Assuming that the excitation temperature for the NH_3 and HCO^+ lines are equal to the kinetic temperature of the envelope, ~ 90 K (see Bujarrabal et al. 1988), we derive column densities of $\lesssim 5 \times 10^{14}$ and $\gtrsim 2 \times 10^{15}$ cm^{-2} for NH_3 and HCO^+, respectively. This gives a NH_3 to HCO^+ abundance ratio of 0.25 and an upper limit to the NH_3 abundance in the envelope of $\lesssim 8 \times 10^{-9}$ for a HCO^+ fractional abundance of 4×10^{-8} (see Bujarrabal et al. 1988). Then, the NH_3 abundance in CRL 618 is at least a factor of 5 smaller than that in IRC +10216 (Nguyen-Q-Rieu, Graham, & Bujarrabal 1984), the prototypical carbon-rich AGB star.

NH_3 in IRC +10216 is believed to form in the transition region between the upper atmosphere of the star and the outer envelope where dust is formed and surface reactions occur (see, e.g., Glassgold 1992). The differences in the NH_3 abundances in the AGB envelopes of CRL 618 and IRC +10216 is probably related to the different physical conditions in this transition layer in both objects. In CRL 618 the transition region between the star and the AGB envelope is probably dominated by the energetic stellar wind and the effects of the strong UV radiation from the central star which also seems to produce important changes in the abundance of other molecules in the envelope (see Bujarrabal et al. 1988).

6. THE CIRCUMSTELLAR DISK IN CRL 618

The strongest evidence for the presence of an anisotropic density distribution around the central star in CRL 618 comes from the bipolar morphology of the H II region (Kwok & Bignell 1984). This density distribution must be the result of

anisotropic mass loss giving rise to a dense circumstellar disk which confines the H II region in declination. The circumstellar disk is expected to be heated by the central star in CRL 618 and it is probably observed as hot dust (Westbrook et al. 1975) and in the HC_3N vibrationally excited emission (Bujarrabal et al. 1988). The hot material observed at extreme blueshifted velocities in NH_3 which is not observed in vibrationally excited HC_3N comes from a different region than the dense and hot circumstellar gas sampled by HC_3N. This would indicate that the bulk of the NH_3 absorption is not related to the circumstellar disk, or the disk has large gradients in molecular abundances coupled with the kinematics, which is unlikely. In addition, the NH_3 velocity gradient across the continuum source is not consistent with the kinematics of a disk rotating around the axis of the molecular outflow, but requires that some material in the disk must be expanding anisotropically at velocities of up 60 km s^{-1}.

The lack of a large disk of hot ammonia in CRL 618 is surprising in view of the spatial distribution of this molecule in a similar PPN, CRL 2688 (Nguyen-Q-Rieu, Weimberg, & Bujarrabal 1986; Truong-Bach, Graham, & Nguyen-Q-Rieu 1988). In this source, all the NH_3 emission arises from a large (0.08 pc × 0.02 pc) disk oriented perpendicularly to the diffuse ionized flow. Since both objects show high-velocity molecular outflows (see Young et al. 1992 for CRL 2688), the main difference between the circumstellar molecular material in CRL 618 and CRL 2688 is again the amount of the UV radiation which impinges on the neutral envelope from the central stars. In CRL 618, the UV field is larger than in CRL 2688 by several orders or magnitude, and ammonia, a very fragile molecule, should be easily photodissociated in the vicinity of the H II region. However, for the typical far-UV radiation field expected for the central star in CRL 618 (B0–O9.5, Westbrook et al. 1975) of 1×10^3–1×10^5 of the interstellar field in units of Habing (1968). NH_3 should be shielded at visual extinction of only 4 mag (see, e.g., Fuente et al. 1991). For the typical densities at the edge of the H II region, $\sim 1 \times 10^7$ cm^{-3}, this corresponds to a distance of only 4×10^{14} cm, beyond which NH_3 should be shielded. If, in the previous stage of evolution CRL 618 would have developed an NH_3 disk similar to that in CRL 2688, most of the NH_3 disk should have survived the intense UV radiation field from the central star. It is very likely that the circumstellar environment of CRL 618 has chemically evolved in a different way than that of CRL 2688.

7. THE BIPOLAR AMMONIA OUTFLOW

The velocity gradient and the line profiles of the NH_3 absorption toward CRL 618 can be explained if NH_3 is present only in the high-velocity molecular outflow. The bipolarity observed in NH_3 is in the same sense as observed in other molecular lines and in the diffuse ionized material (Cernicharo et al. 1989; Neri et al. 1992; Calvet & Cohen 1978). The intersecting area of the blue and redshifted absorption which very likely indicates the location of the central star, occurs, as expected, at the center of the radio continuum emission. The broad NH_3 profiles with the deepest absorption at -50 km s^{-1} are consistent with the sketch in Figure 5. For simplicity, we consider only two components: the AGB expanding envelope with a terminal velocity of 20 km s^{-1} and very low NH_3 abundance, and the high-velocity molecular gas with a large NH_3 abundance. In this scenario a high-velocity primary wind from the central star, very likely already bipolar, interacts with the envelope (expanding at the terminal velocity) modifying the kinematics and the composition of the inner edge of the envelope by shocks. As a consequence, the shocked gas in which NH_3 has been efficiently synthesized is blueshifted to the east and redshifted to the west with respect to the radial velocity of -40 km s^{-1} (radial velocity of the material in the envelope in front of the H II region), producing the observed broad profiles in absorption and the bipolarity (see MB). As pointed out in § 3.2, the NH_3 emission to the side of the H II region cannot be observed with the VLA because of the lack of sensitivity.

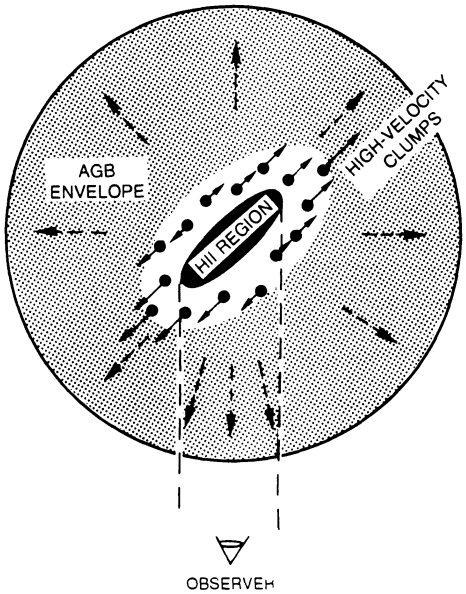

FIG. 5.—Sketch of the model proposed to explain the ammonia profiles toward CRL 618. The size of the H II region (*filled ellipse*) and of the high-velocity molecular clumps (*filled circles*) have been exaggerated with respect to the size of the AGB envelope (*stippled region*). The arrows show the directions of the high-velocity bipolar molecular outflow (*solid*) and of the expanding AGB envelope (*dashed*). The zones of the AGB envelope and of the high-velocity gas sampled by the VLA observations are restricted by the regions contained within the dashed lines.

The NH_3 optical depth maps show, for the first time, the presence of small-scale structure in the high-velocity molecular flow. This corroborates the idea that the molecular flow is produced by the impact of the stellar wind in several clumps. The hot core, with a kinetic temperature of $\gtrsim 270$ K, observed in the high-J metastable lines of NH_3 (see MB) probably represents one of these clumps heated by shocks. The general trend of the optical depth, which increases toward the eastern and western edges of the continuum, indicates that the largest column densities of the high-velocity gas lie outside (at distances of $\gtrsim 0''.2$ from the center) of the H II region. This is consistent with the HCN results which show the maxima of the high-velocity emission at $\sim \pm 1''$ in R.A. from the H II region (Neri et al. 1992).

It is noticeable that the terminal velocity of the bipolar outflow in NH_3, ~ 40 km s^{-1}, is smaller than that of other molecules (~ 200 km s^{-1}). This cannot be due to an excitation effect because the critical densities required to excite the metastable lines of NH_3 are smaller than those of HCN, HC_3N, and HCO^+, and the kinetic temperature measured from NH_3, $\gtrsim 150$ K (see MB), is high enough to excite the (2, 2) line. The low terminal velocities of NH_3 must then be related to the kinematics of the high-velocity gas and/or to the specific chemistry of this molecule in the postshocked gas. The NH_3 data

show some hints of radial velocity changes along the outflow, suggesting that the large flow velocities ($\gtrsim 50$ km s^{-1}) might occur beside the H II region. Acceleration of the high-velocity outflow or a bipolar anisotropic outflow with the velocity as a function of the latitude angle (Bowers 1991) would explain the observed gradient in the radial velocity of the NH_3 data. In the case of acceleration, the molecular outflow must accelerate from 40 to 150 km s^{-1} in only 0.″6 ($\sim 2 \times 10^{16}$ cm). This would be consistent with the HCN measurements (Neri et al. 1992). Though acceleration could explain the low terminal velocities in the absorption lines, it cannot account for the moderate terminal velocities (~ 60 km s^{-1}) of the emission lines observed with single-dish telescopes (see MB). It is then very likely that the chemistry of NH_3 is intimately coupled with the velocity of the outflowing material.

The average optical depth of the NH_3 (2, 2) line at -50 km s^{-1} is 0.28. For a line width of 30 km s^{-1} and an excitation temperature of 150 K, the total column density of NH_3 in the high-velocity gas is $\sim 4 \times 10^{16}$ cm^{-2}. This column density is only a factor of 4 smaller than that derived for the absorption line of HCN (Neri et al. 1992) and the CO to NH_3 abundance ratio is ~ 40. If most carbon is in CO, the fractional abundance of NH_3 in the high-velocity gas, $X(NH_3)$, will be $\sim 2 \times 10^{-5}$ (i.e., 10% of N in NH_3).

8. AMMONIA IN PROTOPLANETARY NEBULAE

Ammonia has been detected in the PPNs CRL 618 (MB), CRL 2688 (Nguyen-Q-Rieu et al. 1984) and OH 231.8+4.2 (Morris et al. 1987). For the PPNs studied in more detail, CRL 618 and CRL 2688, NH_3 does not come from the AGB expanding envelope, but from a hot ($Tk \gtrsim 150$ K) (see Truong-Bach et al. 1988 for CRL 2688; MB for CRL 618) and small region located near the star. The low abundance of this molecule in IRC +10216 (few $\times 10^{-8}$), at least two orders of magnitude smaller than that in CRL 618, indicates that NH_3 must be efficiently synthesized in the postshocked gas left after the interaction of the stellar wind from the central star with the inner part of the AGB envelope. Model calculations of the chemistry in PPNs including the effects of shocks and UV radiation have been made by Howe, Millar, & Williams (1992). The physical conditions in their models are similar to those observed in CRL 618. The results show that significant abundances of a few small molecules are formed in a thin, dense, shocked shell during the first few hundred years of its transition to planetary nebulae. The presence of clumps in the AGB envelope will allow the formation of important amounts of polyatomic molecules. CRL 618 is believed to be in this stage of evolution (see Bujarrabal et al. 1988), and therefore it is very likely that fragile molecules like NH_3 are produced in the shocked clumps. Ammonia will be formed by endothermic reactions between N and H_2. In fact, the NH_3 abundance is strongly enhanced in shocked dense clouds with densities similar to those of the clumps in CRL 618 (Mitchell & Deveau 1983).

9. CONCLUSIONS

Using the VLA, we have made high angular resolution (0.″096 × 0.″066) observations of the radio continuum at 23 GHz and of the ammonia emission of the (2, 2) line toward the PPN CRL 618. The results can be summarized as follows.

1. The contimuun emission is elongated in the east–west direction and shows an elliptical shell structure, reminiscent of an extremely young planetary nebula. While the southern part of the elliptical shell is rather uniform, the northern portion shows clumpy structure. The walls of the shell are unresolved by our 0.″066 beam. The total flux density is similar to that measured after 1980. The continuum structure can be explained if the H II region is not isothermal but the electron temperature increases sharply from 8000 K at the center to 12,000 K in an outer layer of thickness 6×10^{14} cm (0.″020).

2. The (2, 2) line of NH_3 has been detected only in absorption toward the continuum source. The deepest absorption occurs at a radial velocity of -50 km s^{-1} and the line width is ~ 40 km s^{-1}. The absorption lines shows a bipolar distribution with respect to the terminal velocity of the approaching part of the AGB envelope. Absorption with radial velocities $\lesssim -45$ km s^{-1} and $\gtrsim -45$ km s^{-1} are found toward the eastern and the western parts of the H II region, respectively. The data also show hints of acceleration with the more extreme blueshifted velocities appearing at the eastern edge. The line-to-continuum ratios of the absorption lines are not uniform over the continuum, but increase from 0.1 toward the center to 0.4–0.7 toward the eastern and western edges of the H II region.

3. Based on the line profile, the kinematics, and the spatial distribution of the NH_3 absorption line, we show that the NH_3 absorption does not arise from the AGB envelope but from the postshocked material left after the interaction of the primary wind from the central star with the inner parts of the AGB envelope.

4. We derive an NH_3 fractional abundance of less than 8×10^{-9} in the AGB envelope and larger than 2×10^{-5} in the high-velocity molecular outflow. We propose that the enhancement of the ammonia abundance by more than three orders of magnitude in the high-velocity outflows is produced by shock chemistry.

This work has been partially supported by the Spanish CICYT under grant PB90-408. J. M.-P. and R. G. have been partially supported by the NATO grant 900440.

REFERENCES

Bachiller, R., Gómez-Gonzalez, J., Bujarrabal, V., & Martín-Pintado, J. 1988, A&A, 196, L5
Beckwith, S., Beck, S. C., & Gatley, I. 1984, ApJ, 280, 648
Bowers, P. F. 1991, ApJS, 76, 1099
Bujarrabal, V., Gómez-González, J., Bachiller, R., & Martín-Pintado, J. 1988, A&A, 204, 242
Burton, M. G., & Geballe, T. R. 1986, MNRAS, 223, 13P
Calvet, N., & Cohen, M. 1978, MNRAS, 182, 687
Carsenti, U., & Solf, J. 1982, A&A, 106, 307
Cernicharo, J., Guélin, M., Martín-Pintado, J., Peñalver, J., Mauersberger, R. 1989, A&A, 222, L1
Fuente, A., Martín-Pintado, J., Cernicharo, J., & Bachiller, R. 1991, A&A, 237, 471
Gammie, C. F., Knapp, G. R., Young, K., Phillips, T. G., & Falgarone, E. 1989, ApJ, 345, L87
Glassgold, A. E. 1992, in IAU Symp. 150, The Astrochemistry of Cosmic Phenomena, ed. P. D. Singh, in press
Habing, H. J. 1968, Bull. Astron. Inst. Netherlands, 19, 421
Howe, D. A., Millar, T. J., & Williams, D. A. 1992, MNRAS, 255, 217
Kwok, S., & Bignell, R. C. 1984, ApJ, 276, 540
Kwok, S., & Feldman, P. A. 1981, ApJ, 267, L67
Martín-Pintado, J., & Bachiller, R. 1992, ApJ, 391, L93 (MB)
Martín-Pintado, J., Bujarrabal, V., Bachiller, R., Gómez-González, J., & Planesas, P. 1988, A&A, 197, L15
Mitchell, G. F., & Deveau, T. J. 1983, ApJ, 266, 646
Morris, M., Guilloteau, S., Lucas, R., & Omont, A. 1987, ApJ, 321, 888

Neri, R., García-Burillo, S., Cernicharo, J., Guélin, M., Guilloteau, S., & Lucas, R. 1992, A&A, 262, 554
Nguyen-Q-Rieu, Graham, D., & Bujarrabal, V. 1984, A&A, 138, L5
Nguyen-Q-Rieu, Weimberg, A., & Bujarrabal, V. 1986, A&A, 165, 204
Osterbrock, D. E. 1989, Astrophysics of Gaseous Nebulae and Active Galactic Nuclei (Mill Valley, CA: University Science)
Pottasch, S. R. 1984, Planetary Nebulae (Dordrecht: Reidel)
Rubin, R. H. 1968, ApJ, 153, 761
Spergel, D. N., Giuliani, J. L., Jr., & Knapp, G. R. 1983, ApJ, 275, 330
Truong-Bach, Graham, D., & Nguyen-Q-Rieu, 1988, A&A, 199, 291
Walmsley, M., Chini, R., Kreysa, E., Steppe, H., Forveille, T., & Omont, A. 1989, A&A, 248, 555
Westbrook, E. E., Becklin, K. M., Merril, K. M., Neugebauer, G., Schmidth, S. P., & Wynn-Williams, C. G. 1975, ApJ, 202, 407
Young, K., Serabyn, E., Phillips, T. G., Knapp, G. R., Güsten, R., & Schulz, A. 1992, ApJ, 385, 265
Zuckermann, B., Palmer, P., Turner, B. E., Gilra, D. P., Bowers, P. F., & Gilmore, W. S. 1977, ApJ, 211, 197